

2. Armbrecht JJ, Buxton DB, Schelbert HR. Validation of [ $^{11}\text{C}$ ] acetate as a tracer for noninvasive assessment of oxidative metabolism with positron emission tomography in normal, ischemic, posts ischemic, and hyperemic canine myocardium. *Circulation* 1990;81:1954-1605.
3. Brown M, Marshall DR, Sobel BE, Bergmann SR. Delineation of myocardial oxygen utilization with carbon-11-labeled acetate. *Circulation* 1987;76:687-96.
4. Brown MA, Myers DW, Bergmann SR. Noninvasive assessment of canine myocardial oxidative metabolism with carbon-11-acetate and positron emission tomography. *J Am Coll Cardiol* 1988;12:1054-1063.
5. Brown MA, Myers DW, Bergmann SR. Validity of estimates of myocardial oxidative metabolism with carbon-11-acetate and positron emission tomography despite altered patterns of substrate utilization. *J Nucl Med* 1989;30:187-93.
6. Buxton DB, Schwaiger M, Nguyen A, Phelps ME, Schelbert HR. Radio-labeled acetate as a tracer of myocardial tricarboxylic acid cycle flux. *Circ Res* 1988;63:628-34.
7. Buxton DB, Nienaber CA, Luxen A, Ratib O, Hansen H, Phelps ME, Schelbert HR. Noninvasive quantitation of regional myocardial oxygen consumption in vivo with [ $^{11}\text{C}$ ] acetate and dynamic positron emission tomography. *Circulation* 1989;79:134-42.
8. Henes CG, Bergmann SR, Walsh MN, Sobel BE, Geltman EM. Assessment of myocardial oxidative metabolic reserve with positron emission tomography and carbon-11-acetate. *J Nucl Med* 1989;30:1489-99.
9. Heyman M, Payne B, Hoffman J, Rudolph A. Blood flow measurements with radionuclide-labeled particles. *Prog Cardiovasc Dis* 1977;20:55-79.
10. Gambhir SS, Schwaiger M, Huang SC, Krivokapich J, Schelbert HR, Nienaber CA, Phelps ME. Simple noninvasive quantification method for measuring myocardial glucose utilization in humans employing positron emission tomography and fluorine-18-deoxyglucose. *J Nucl Med* 1989;30:359-66.
11. Randle PJ, England PJ, Denton RM. Control of the tricarboxylate cycle and its interactions with glycolysis during acetate utilization in rat heart. *Biochem J* 1970.
12. Ng C, Huang HR, Schelbert HR, Buxton DB. A kinetic model for C-11-acetate as a tracer for myocardial oxidative metabolism. *J Nucl Med* 1990;31:1581.

## EDITORIAL

# Relationship Between Myocardial Clearance Rates of Carbon-11-Acetate-Derived Radiolabel and Oxidative Metabolism: Physiologic Basis and Clinical Significance

### APPROACHES TO IMAGING MYOCARDIAL METABOLISM

Unlike the brain, which normally utilizes glucose as its primary metabolic substrate, the heart relies on a variety of substrates for energy production. In fact, under baseline conditions, glucose metabolism accounts for only about half of all cardiac substrate metabolism, and this value can decrease with decreases in blood-glucose levels. Therefore, while fluorodeoxyglucose (FDG), a glucose analog, is the standard tracer for quantifying cerebral metabolism and for imaging cerebral function with PET, it cannot be used to estimate cardiac energy production. Even the regional patterns of FDG-derived radiolabel accumulation do not necessarily reflect the patterns of regional cardiac energy production qualitatively (1-3).

Researchers have therefore had to seek other potential metabolic tracers in efforts to find a method of imaging metabolism in the heart. For example, radiolabeled fatty acids have been ex-

plored as metabolic tracers, but fatty acid metabolism accounts for only 40%-80% of overall cardiac energy production under normal conditions and is highly variable. Radiolabeled molecular oxygen has been used to image brain oxidative metabolism, but technical difficulties have prevented its use in the heart.

Recently, the use of some radiolabeled analogs of acetate has been suggested as an approach to image myocardial oxidative metabolism. Acetate is rapidly converted into acetylcoenzyme A (acetyl CoA) in the heart and acetyl CoA is the link between Krebs cycle oxidative metabolism and the initial metabolism of glucose, fatty acids, lactate, and protein. The possibility of using an acetate analog to map overall oxidative metabolism is therefore inviting.

Interestingly, the relationship between acetate and its fluorinated derivative, fluoroacetate, at first resembles that of glucose and fluorodeoxyglucose. FDG is metabolized to FDG-6-phosphate as glucose is metabolized to glucose-6-phosphate, but further FDG-6-phosphate metabolism is very slow and therefore it accumulates in proportion to the rate of glucose me-

tabolism (4,5). Similarly, fluoroacetate is metabolized to fluorocitrate as acetate is metabolized to citrate, with further metabolism of fluorocitrate being extremely slow. Unfortunately, the analogy ends here. Fluoroacetate kinetics are very different from acetate kinetics (6), and fluorocitrate is an extremely potent metabolic poison. Thus, fluoroacetate has not found use as a metabolic tracer.

### RADIOLABELED ACETATE AS A METABOLIC TRACER

Investigators have had better luck with the use of radiolabeled acetate (ACE) itself as a metabolic tracer. Following intravenous administration, ACE is converted into ACE-CoA in heart cells by a rapid and poorly regulated process (7,8). The ACE-CoA is subsequently metabolized through the Krebs cycle with the radiolabel being lost as  $\text{CO}_2$ . Because ACE can be labeled with positron-emitting  $^{11}\text{C}$ , and because regional cardiac  $^{11}\text{C}$  activity over time can then be imaged with PET scanners, the use of  $^{11}\text{C}$ -ACE in PET imaging of cardiac metabolism has been investigated.

Preliminary studies suggested an

Received Dec. 21, 1990; revision accepted Jan. 29, 1991.

For reprints contact: James L. Lear, MD, Nuclear Medicine (A034), UCHSC, 4200 E. 9th Ave., Denver, CO 80262.

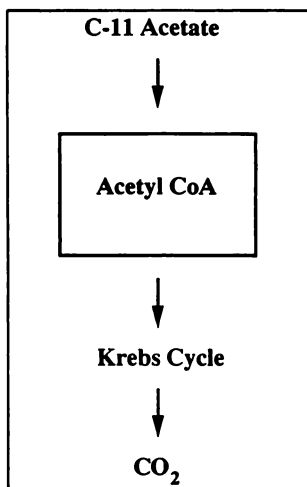


**FIGURE 1.** It was originally proposed that  $^{11}\text{C}$ -acetate was rapidly converted into a pool of  $^{11}\text{C}$ -acetyl CoA, which was then metabolized in a step-wise manner directly through the Krebs cycle.

apparent relationship between  $^{11}\text{C}$  tissue clearance rates and oxygen metabolism in normal animals (9,10). Based on data from these studies, a mathematical model and its related experimental technique were developed in an effort to quantify rates of myocardial oxygen metabolism under various conditions using PET-measured clearance rates of ACE-derived  $^{11}\text{C}$  (8,11-17).

The model assumes that ACE is converted into ACE-CoA within a few minutes of administration (Fig. 1). The ACE-CoA therefore represents a metabolic pool containing the radiolabel and this pool is cleared through the Krebs cycle (8). If the regional myocardial radiolabel activities are plotted versus time (beginning a few minutes after tracer administration), then exponential decay curves can be fit to the data and clearance rate constants ( $k^{-1}$ ) can be determined. These rate constants of radiolabel clearance from the myocardium are presumed to reflect the regional Krebs cycle metabolic rates.

Such rate constants were determined in series of normal subjects and correlated with independently meas-

ured oxygen metabolic rates. A factor was then derived relating the clearance-curve rate constants of the ACE-derived radiolabel to oxygen metabolic rates:

$$R = k^{-1}/\text{MRO}_2$$

where  $R$  = correlation factor,  $k^{-1}$  = rate constant of ACE-derived radiolabel clearance-curve, and  $\text{MRO}_2$  = myocardial oxygen metabolic rate.

Two major assumptions have been applied to this factor,  $R$ .

1.  $R$  has been assumed to be a physiologic constant, i.e., the value determined for normal subjects applies to other subjects.
2. It has also been assumed that  $R$  values measured from experimental studies using intra-arterial tracer injections apply to clinical studies using intravenous injections.

Thus, it has been suggested that, after  $R$  has been determined under controlled conditions, it can be used to convert PET-measured clearance rates of ACE-derived radiolabel from other physiologic and pathologic conditions of interest into corresponding oxygen metabolic rates. Both of these assumptions need critical examination.

## PHYSIOLOGIC BASIS OF RELATIONSHIP BETWEEN ACE-DERIVED RADIOLABEL CLEARANCE RATES AND OXIDATIVE METABOLISM

A recent analysis of data from several studies has shown that the radiolabeled acetyl CoA concentration in heart cells is far too small, less than 1/1000 the necessary value, for ACE-CoA to represent the predominant metabolic compartment containing the ACE-derived  $^{11}\text{C}$  (1). Also, the Krebs cycle is not a specific chain of one directional metabolic steps. Rather, it is a complex series of chemical reactions having complex side-branches, which for simplicity can be represented as a self-renewing cycle of intermediate metabolites.

Therefore, a different model is needed to explain the relationship between  $^{11}\text{C}$  tissue clearance and oxygen metabolism (Fig. 2). Carbon-11-ACE is rapidly metabolized into  $^{11}\text{C}$ -ACE-CoA that rapidly enters the Krebs cycle. During the two or three trips through the cycle that are required before the labeled carbon atom can begin to be lost to  $\text{CO}_2$ , the label can distribute among the Krebs cycle intermediate substrates and can also enter the related amino acid pools through the action of transaminases (1,7,18). The pool from which the  $^{11}\text{C}$  is eventually lost via metabolism into  $\text{CO}_2$  is therefore much greater in size

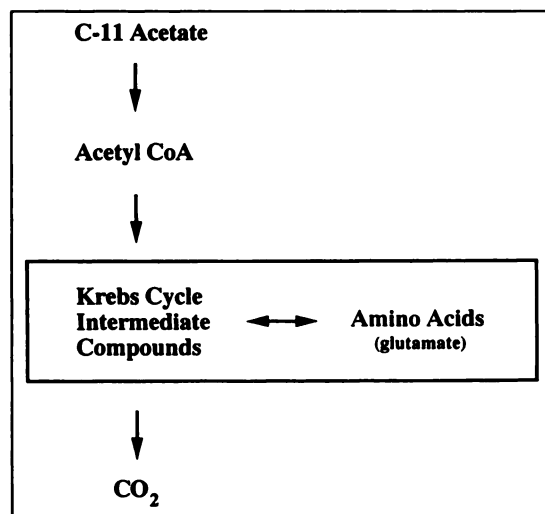


**FIGURE 2.** As opposed to the model shown in Figure 1,  $^{11}\text{C}$  distributes among the various intermediate metabolites of the Krebs cycle as well as related amino acids, predominantly glutamate. After reaching equilibrium, the label clears from this much larger group of metabolic pools. The rate of radiolabel clearance reflects the ratio of the Krebs cycle flux divided by the effective sum of the metabolic pool sizes, not the rate of Krebs cycle flux alone.

and complexity than the small acetyl CoA pool. Calculations of the effective size of the total ACE-derived radiolabel pool indicate that it is equal to the sum of the sizes of the Krebs cycle intermediate substrate pools plus a large fraction of the glutamate pool (1). In fact, within a few minutes of tracer administration, glutamate, as opposed to the Krebs-cycle compounds themselves, is probably the most important metabolic pool containing the ACE-derived radiolabel.

What are the effects of this important change in the model from which the ACE-based technique for quantifying cardiac oxidative metabolism was derived? First, the simple "first in, first out" concept that has been applied to the pathway of the radiolabel is inaccurate. Second, the actual size of the metabolic compartment from which the  $^{14}\text{C}$  clears becomes critical, because *the rate constant of the clearance curve ( $\text{min}^{-1}$ ) is not equal to the Krebs cycle flux ( $\text{mmol g}^{-1} \text{min}^{-1}$ ), but rather, is equal to the ratio of the Krebs cycle flux divided by the effective size ( $\text{mmol g}^{-1}$ ) of the group of metabolite pools into which the radiolabel has become distributed.*

Therefore, while changes in the rate of Krebs cycle flux will change the slopes of  $^{14}\text{C}$  clearance curves, *effects which are similar in magnitude but opposite in direction can be produced independently by changes in the sizes of the  $^{14}\text{C}$  distribution pools.* Unless the sizes of the metabolic pools in a given condition are accurately known, one cannot calculate oxygen metabolic rates from  $^{14}\text{C}$  clearance-curve rate constants. As the complexity of the metabolic pools into which the  $^{14}\text{C}$ -derived from ACE distributes is just becoming appreciated, it is premature to conclude that their individual sizes or the sum of their sizes are fixed across all species or all physiologic and pathologic conditions within a species.

In fact, some recent comparisons of ACE-derived radiolabel clearances under fasting and non-fasting conditions could be explained by such variations in the size of the  $^{14}\text{C}$  metabolic

pools (17). The authors found significantly greater  $^{14}\text{C}$  clearance rates and therefore they calculated significantly greater oxidative metabolic rates in the hearts of patients given fatty acid infusions compared to rates in the hearts of control patients. This unexplained phenomenon occurred despite the fact that the average rate-pressure product, which largely determines cardiac oxygen consumption, was lower in the patients given the fatty acid infusions than in the control patients. This observation could be explained by a decrease in the size of the  $^{14}\text{C}$  pool in the patients given fatty acids, rather than an increase in their rate of cardiac oxidative metabolism. Discordances between reported ACE clearance rates and rate-pressure products in fasted versus control patients (17) could be explained similarly.

#### **EFFECTS OF INPUT FUNCTION PROLONGATION CAUSED BY INTRAVENOUS TRACER ADMINISTRATION**

It has been assumed that, after the ACE-derived myocardial radiolabel concentration has peaked (a few minutes following the ACE administration), the subsequent time course of activity is determined by the loss of radiolabel through  $\text{CO}_2$  production. Other factors such as washout of unmetabolized ACE from the myocardium or continuing uptake of ACE by the myocardium from the plasma are considered to be negligible.

This assumption is reasonable with intracoronary administrations of ACE. A portion of the ACE which enters the myocardium is rapidly metabolized and trapped as ACE-CoA. The remainder is rapidly washed out before being metabolized and is gone within a few minutes. The amount of ACE that recirculates and later enters the myocardium is very small compared to the original input function. Thus, loss of radiolabel through  $\text{CO}_2$  production becomes the main determinant of the myocardial time-activity curve within a short time of the ACE administration.

However, the study by Buck et al. (19) in this issue suggests that this assumption may not be true with intravenous injections, the type employed in most clinical studies. Following intravenous administration, the concentration of ACE in the plasma rapidly decreases (6), but may not reach negligible levels by the time that the myocardial clearance measurements are begun. Thus, some "new" ACE can enter the heart as the "old" ACE is being metabolized and lost as  $\text{CO}_2$ . This continuing input function will alter the observed radiolabel clearance curves slightly. Buck et al. have proposed that the ACE-derived radiolabel clearance curves should be corrected for the small but persistent input function and have developed a model to do so (19). Using the new model, they have reported significantly better data fits in patients to whom the  $^{14}\text{C}$ -acetate was administered intravenously rather than intra-arterially.

#### **CLINICAL IMPLICATIONS**

Despite the above problems, cardiac clearance rate images of ACE-derived  $^{14}\text{C}$  have been found to be similar between different normal patients under controlled conditions. Also, clearance rate images have shown interesting patterns in patients with infarctions and ischemia. Therefore, problems with estimating actual oxygen metabolic rates from ACE-derived  $^{14}\text{C}$  clearance rates do not necessarily imply problems with the use of ACE imaging for clinical purposes. While ACE imaging would have obvious clinical utility if it directly reflected regional oxidative metabolism, clinical utility does not depend upon a direct correlation between ACE-derived radiolabel clearance rates and oxygen metabolic rates. The effects on clinical diagnoses of errors in metabolic measurements using ACE will be determined by how the errors interact with parameters of clinical importance rather than by how they influence physiologic measurements.

Variations in ACE-derived radiolabel distribution spaces could have pos-

itive or negative effects on diagnostic utility, depending upon whether the errors amplify or diminish clinically significant signals. For example, if ischemia causes the ACE-derived radiolabel distribution space to increase, then the ability to detect coronary artery disease could be enhanced because the clearance curves would be prolonged by both the decreased metabolism and the increased distribution-space size. On the other hand, if ischemia were to decrease the size of the distribution space, then the decrease in  $^{11}\text{C}$  clearance rates caused by the ischemia could be masked by the increase caused by the alteration in the distribution-space size.

The effects on clinical diagnoses of the failure to correct radiolabel clearance rate images for the small levels of circulating ACE are also uncertain. If the time course of plasma-ACE levels tends to be constant between patients, then a small residual level will cause only a small systematic prolongation of the clearance curves, and would thus not affect diagnostic utility. However, if the input functions vary significantly between patients, then diagnostic accuracy could be affected.

In summary, the potential for using clearance rates of ACE-derived  $^{11}\text{C}$  in PET imaging of myocardial oxidative metabolism remains intriguing. However, more investigative and comparative work needs to be performed before definite conclusions can be drawn regarding the link between ra-

diolabel clearance rates and myocardial oxidative metabolism or the clinical status of the heart.

#### ACKNOWLEDGMENTS

Supported by a Scholar grant of the Radiological Society of North America and by NIH grant NS-26657.

James L. Lear

University of Colorado Health Sciences

Center

Denver, Colorado

#### REFERENCES

- Lear JL, Ackermann RF. Quantification of patterns of regional cardiac metabolism. *Radiology* 1990;176:659-664.
- Gropler RJ, Siegel BA, Lee KJ, et al. Nonuniformity in myocardial accumulation of fluorine-18-fluorodeoxyglucose in normal fasted humans. *J Nucl Med* 1990;31:1749-1756.
- Schwaiger M, Hicks R. Regional heterogeneity of cardiac substrate metabolism. *J Nucl Med* 1990;31:1757-1759.
- Sokoloff L, Reivich M, Kennedy C, et al. The [ $^{14}\text{C}$ ]deoxyglucose method of local cerebral glucose utilization: theory, procedure, and normal values in the conscious and anesthetized albino rat. *J Neurochem* 1977;28:897-916.
- Phelps M, Hoffman E, Selin C, et al. Investigation of [ $^{18}\text{F}$ ]2-fluoro-2-deoxyglucose for the measure of myocardial glucose metabolism. *J Nucl Med* 1978;19:1311-1319.
- Lear J, Ackermann R. Evaluation of radiolabeled acetate and fluoroacetate as potential tracers of cerebral oxidative metabolism. *Metabolic Brain Dis* 1990;5:45-56.
- Randle P, England P, Denton R. Control of the tricarboxylate cycle and its interactions with glycolysis during acetate utilization in rat heart. *Biochem J* 1970;117:677-695.
- Brown M, Myears D, Bergmann S. Validity of estimates of myocardial oxidative metabolism with carbon-11-acetate and positron emission tomography despite altered patterns of substrate utilization. *J Nucl Med* 1989;30:187-193.
- Brown M, Marshall D, Sobel B, Bergmann S. Delineation of myocardial oxygen utilization with carbon-11-labeled acetate. *Circulation* 1987;76:687-696.
- Buxton D, Schwaiger M, Nguyen A, et al. Radiolabeled acetate as a tracer of myocardial tricarboxylic acid cycle flux. *Circ Res* 1988;63:628-634.
- Brown MA, Myears DW, Bergmann SR. Noninvasive assessment of canine myocardial oxidative metabolism with carbon-11-acetate and positron emission tomography. *J Am Coll Cardiol* 1988;12:1054-1063.
- Walsh M, Geltman E, Brown M, et al. Noninvasive estimation of regional myocardial oxygen consumption by positron emission tomography with carbon-11-acetate in patients with myocardial infarction. *J Nucl Med* 1989;30:1798-1808.
- Armbrecht JJ, Buxton DB, Brunken RC, et al. Regional myocardial oxygen consumption determined non-invasively in humans with [ $^{11}\text{C}$ ]acetate and dynamic positron tomography. *Circulation* 1989;80:863-872.
- Henes CG, Bergmann SR, Walsh MN, et al. Assessment of myocardial oxidative metabolic reserve with positron emission tomography and carbon-11-acetate. *J Nucl Med* 1989;30:1489-1499.
- Buxton DB, Nienaber CA, Luxen A, et al. Noninvasive quantitation of regional myocardial oxygen consumption in vivo with [ $^{11}\text{C}$ ]acetate and dynamic positron emission tomography. *Circulation* 1989;79:134-142.
- Armbrecht JJ, Buxton DB, Schelbert HR. Validation of [ $^{11}\text{C}$ ]acetate kinetics as a tracer for noninvasive assessment of oxidative metabolism with positron emission tomography in normal, ischemic, postischemic, and hyperemic canine myocardium. *Circulation* 1990;81:1594-1605.
- Kotzerke J, Hicks RJ, Wolfe E, et al. Three-dimensional assessment of myocardial oxidative metabolism: a new approach for regional determination of PET-derived carbon-11-acetate kinetics. *J Nucl Med* 1990;31:1176-1183.
- Chance E, Seeholzer S, Kobayashi K, Williamson J. Mathematical analysis of isotope labeling in the citric acid cycle with applications to  $^{13}\text{C}$  NMR studies in perfused rat hearts. *J Biol Chem* 1983;258:13785-13794.
- Buck A, Wolpers HG, Hutchins GD, et al. Tracer kinetic modeling of myocardial [ $^{11}\text{C}$ ]acetate kinetics. *J Nucl Med* 1991;32:1950-1957.